A Study of Polysulfide Sealants for Joints in Bridges

JOHN P. COOK
Assistant Professor of Civil Engineering, Rensselaer Polytechnic Institute

The polysulfide sealants used in expansion joints in bridges are commonly assumed to be perfectly elastic materials. This paper shows that these sealants are acutally viscoelastic and exhibit the interrelated phenomena of creep and stress relaxation. Curves are included for modulus of elasticity, creep, and stress relaxation, with shape factor, Shore hardness and temperature as parameters. Sample solutions are shown for the stresses in the sealants under various loading conditions, including tension plus shear and compression plus shear. A stress relaxation equation is derived using a curve-fitting technique and the stress relaxation relationship is verified by standard laboratory methods and by the method of photoelasticity.

•THE ENGINEER or scientist today, in dealing with the properties and behavior of solid materials, generally has at his command theories which, if not perfect, are at least acceptable and consistent. The engineer who worked with rubber-like materials had until recently no such assurance. It remained for the chemist and physicist correctly to postulate certain properties of highly extensible molecules before consistent theories were developed.

Although much of the significant work in this field has been done in recent years, the problem dates back almost 100 years and shows three distinct roots:

1. The general problem of flow in solid materials, beginning with the work of J. C. Maxwell;
2. Research in the field of rubber-like materials by such investigators as Treloar, Kuhn, Guth, Rivlin, and Tobolsky, dating back roughly 25 years; and
3. Specific works in the field of joint sealants, notably that by Tons (1).

Recent papers have shown a very intimate relation between the first two of these roots in the effort to explain the behavior of various polymers, including the polysulfide rubbers. Outside of Tons' work, very little effort has been made to apply this earlier work to the specific problem of expansion joints.

A study of this history brings two cases into focus, the perfectly elastic sealant and the material which flows with time. Since the polysulfide sealant can be formulated with a wide range of properties, both of these cases should be considered.

A joint sealant may fail mechanically in any one of the several ways shown in Figure 1:

1. The adhesive failure is a loss of bond between the sealant and the joint wall caused by a tensile load. It may start as a small localized failure and then peel rather rapidly under the action of stress.
2. The cohesive failure is a tearing of the sealant material, also under tension.
3. The extrusion failure occurs under the combined action of compression and traffic. The material under compression is extruded above the roadway surface and then folded and flattened under the action of traffic.

Paper sponsored by Committee on Sealants and Fillers for Joints and Cracks in Pavements and presented at the 43rd Annual Meeting.

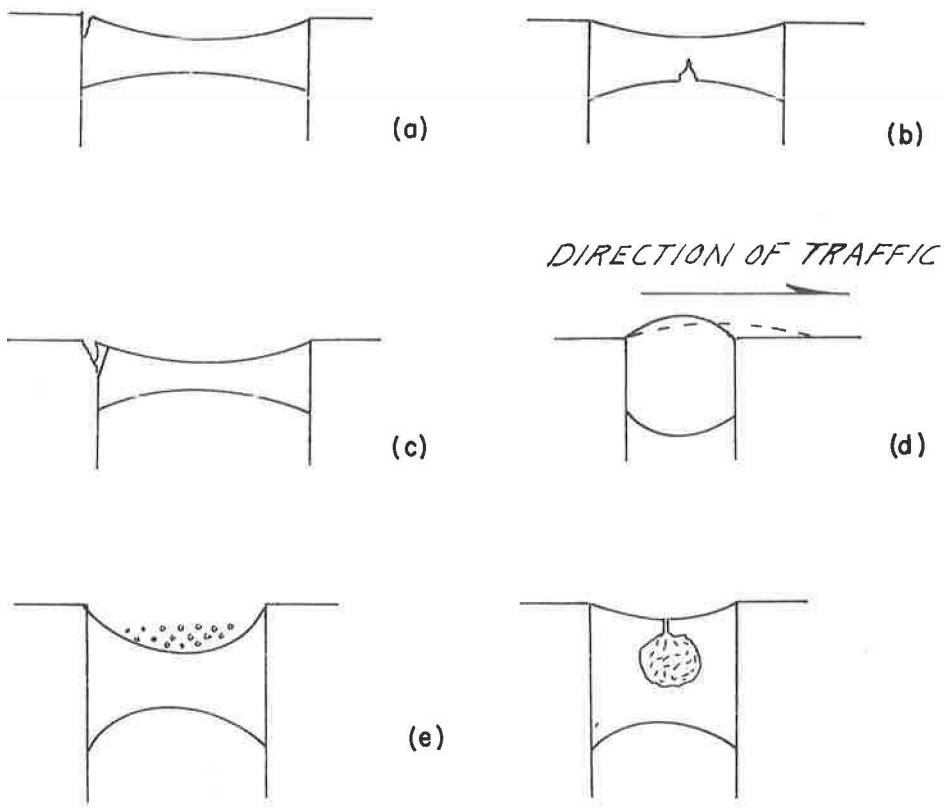

Figure 1. Types of joint failures: (a) adhesion, (b) cohesion, (c) spalling, (d) extrusion, and (e) intrusion.

4. The spalling failure is not, strictly speaking, a sealant failure, but its effect is just as destructive. In this case, the concrete adjacent to the joint interface spalls, generally under the action of heavy traffic, and the salt solution leaks past the sealant. The spalling failure is generally localized in the primary traffic lane but it breaks the continuity of the joint and quite often leads to a general peel-type adhesive failure.

5. The intrusion failure occurs under the combined action of extension and traffic. The sealant under tension necks down, forming a pocket, which fills with dirt. As the joint closes, this dirt is trapped within the sealer mass. This weak spot usually leads to a cohesive failure during the next extension cycle.

These failures are described in the literature. However, the present work demonstrates the extent of stress relaxation in the sealant, so two more failures attributable in large part to flow and stress relaxation are shown in Figure 2.

In each of the two cases shown in Figure 2, the sealant is loaded in normal fashion (either tension or compression) and then held at constant deformation until some degree of stress relaxation has taken place. On the next return cycle it begins deforming from this new shape and does not return to the original rectangle. In each case, a failure is imminent with additional cycling.

All these potential failures are accelerated by the effects of aging and weathering. However, the manufacturers of the various sealant materials are constantly striving to improve these products in their resistance to weather, salts, acids and solvents, so the effects of weathering will recieve no treatment here.

Each of the failure conditions mentioned presents a separate problem and the solutions may vary quite markedly, depending on the field conditions. The attempt being

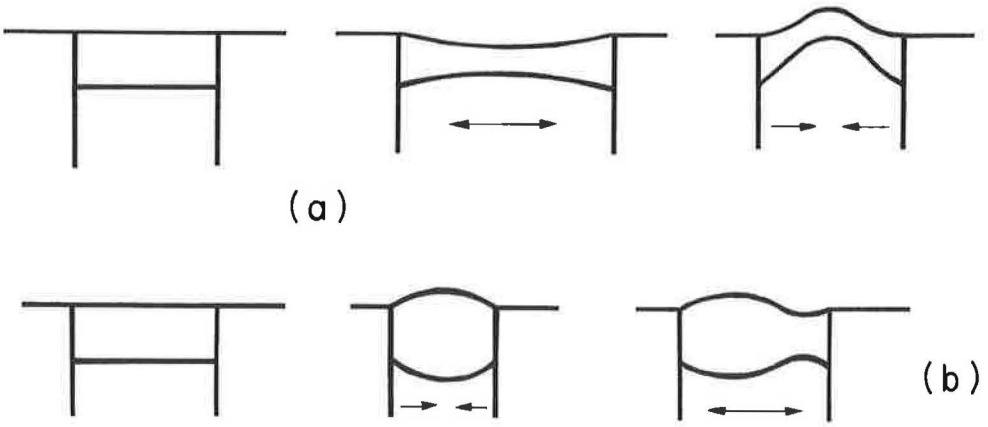

Figure 2. Change in sealant shape due to flow: (a) viscous tension-compression effect, and (b) viscous compression-tension effect.

made here is not to provide field solutions for all these problems but to evaluate the polysulfide sealant material; in the course of this investigation, the solutions of some of these cases present themselves.

PURPOSE OF STUDY

The purpose of this study was to consider the polysulfide sealant first as a perfectly elastic material and then as a flowing solid and to determine what stresses exist under load in a bridge joint. Inherent in this search, of course, was the determination of modulus and, what is more important, of the proper relationship between stress, modulus and strain, with time, temperature, shape factor and extensibility as the necessary parameters. Experimental work in this study included those tests which were necessary to establish the parametric relationships.

Appendix B of this paper includes sample solutions for the stresses in the sealant as follows: (a) considering the sealant as a perfectly elastic material--tension (or compression) alone, tension plus shear, and tension plus end rotation of the structure as caused by midspan deflection; and (b) considering the sealant as a flowing solid--tension (or compression) as caused by an imposed strain program corresponding to bridge movement.

THEORY

Sealant as a Perfectly Elastic Material

Many formulas have been presented in the attempt to show the proper relationship between stress, modulus and strain. Some have used the classical approach through the theory of rubber elasticity, and others have used an empirical approach. Treloar (2) has summed up the work of previous investigators and, working with an acceptable molecular model, has developed the kinetic theory expression in terms of extension ratios and the familiar shear modulus. The approach, which is made on a statistical basis using the entropy method, is explainable in terms of a mechanical model and lends itself to extension to the case in which the flow properties of the material are considered.

The internal work of deformation within a joint sealant according to Treloar's Kinetic Theory is expressed as:

$$W = \tfrac{1}{2} G \left[\lambda_1^2 + \lambda_2^2 + \lambda_3^2 - 3 \right] \qquad (1)$$

in which G is shear modulus and λ is ratio of extended length to the original dimension, in each of three directions. The external work done by the applied forces is

$$dW = f_1 d\lambda_1 + f_2 d\lambda_2 + f_3 d\lambda_3 \quad (2)$$

Differentiating the internal work expression and equating it to the external work expression yields a set of simultaneous equations:

$$\begin{aligned} \lambda_1 f_1 - \lambda_3 f_3 &= G(\lambda_1^2 - \lambda_3^2) \\ \lambda_2 f_2 - \lambda_3 f_3 &= G(\lambda_2^2 - \lambda_3^2) \end{aligned} \quad (3)$$

These are the general stress-strain relations which hold within the range of the Gaussian probability function on which Treloar's statistical derivation is based. Practically speaking, these formulas are valid up to approximately 200 percent extension in the sealant.

These equations simplify when applied to the joint sealant problem because the joint extends across two or three lanes of traffic and, hence, has a length in this direction of 30 to 40 ft as compared to cross-sectional dimensions of approximately 1 in. With no loss of generality the extension ratio in this transverse direction can always be considered as unity.

Since the sealant undergoes no change in volume the following relationship must hold true:

$$\lambda_1 \lambda_2 \lambda_3 = 1 \quad (4)$$

Therefore, for a sealant under simple elongation the extension ratios are $\lambda_1 = \lambda$, $\lambda_2 = 1/\lambda$, and $\lambda_3 = 1$.

Since the only external force acting on the sealant is in the tensile (λ_1) direction, the stress reduces to:

$$f = \frac{dW}{d\lambda} = G\left[\lambda - \frac{1}{\lambda^3}\right] \quad (5)$$

Sealant as a Flowing Solid

In macroscopic terms, the viscoelastic behavior of polymers is usually separated into three components, instantaneous elasticity, delayed elasticity and viscous flow. Billmeyer (3) associates these properties with molecular structure as follows:

1. Instantaneous elasticity--stretching of the primary valence bonds and straightening of the bond angles in the main polymer chain (a reversible action);
2. Delayed elasticity--reversible uncoiling of the polymer chains and orienting them in the direction of the stress; and
3. Viscous flow--irreversible slipping of the chains past one another.

These actions are, of course, stated in completely general terms and the interrelation between them is a function of other parameters such as temperature.

To the laboratory observer, the essential difference between the elastic and the viscoelastic body is that the latter shows the two interrelated phenomena of creep and stress relaxation. Both of these phenomena are capable of explanation in terms of molecular structure. The mechanism of creep, which is demonstrated later, becomes apparent when a creep curve is shown together with the model movements which represent the behavior.

The method of analogous mechanical models has been selected for use in this present work because it defines the behavior of the material in a manner which can be logically explained in terms of the molecular structure of the polymer. The method is said to be an approximation but Billmeyer (3) and many others feel that because of its sound basis in molecular theory, it offers the best solution currently available.

The model method consists of the identification of molecular behavior with certain types of response to an applied stress. These responses are then represented by simple mechanical models which can be explained in mathematical terms. An ideally elastic material is represented by a spring, which obeys Hooke's law, that is, stress proportional to strain (Fig. 3). A completely viscous response is represented by the hydraulic dashpot (Fig. 4). For this element, stress is proportional to strain rate. The third basic element, the friction unit, shows no movement until stress reaches some limiting value represented as a friction force (Fig. 5).

Certain basic combinations of these units occur so often that these combinations are considered almost as elements. The series combination of a spring and a dashpot is known as a Maxwell model (Fig. 6) and represents a material which shows an instantaneous elasticity and a straight-line creep under load and some amount of flow or permanent set on removal of the load. The parallel combination of a spring and a dashpot is known as a Kelvin (or Voigt) unit (Fig. 7), which represents a material displaying a damped or delayed elasticity under load but no permanent set on removal of the load.

Figure 3. Model for ideally elastic material.

Figure 4. Model for viscous flow.

Figure 5. Friction model.

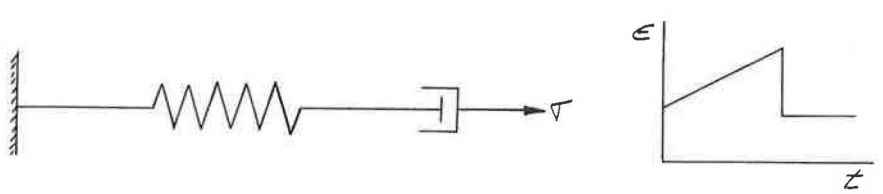

Figure 6. Maxwell model.

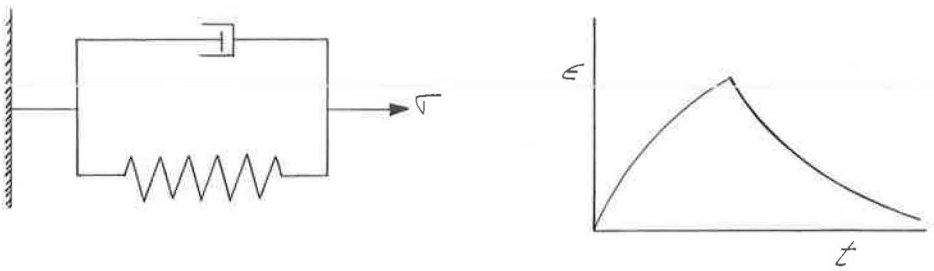

Figure 7. Kelvin model.

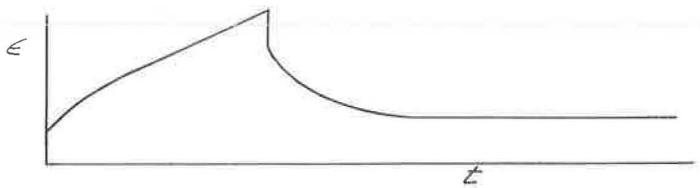

Figure 8. General creep curve.

To describe a material with a model system we must know which basic elements are present and what combinations exist. A creep curve (strain vs time at constant load) for the material in question will generally establish the presence of springs and dashpots in a system. The friction element can be identified by plotting various load-increment curves of elongation vs time.

The creep curve for the polysulfide rubbers, shown in Figure 8, duplicates the curve shown in many texts as the generalized curve for all rubbery polymers. Comparison of this curve with the creep curves of the Maxwell and Kelvin units immediately suggests an additive combination of the Maxwell and Kelvin units with a four-element model to describe material behavior. The presence of a yield point (friction unit) is ruled out by creep tests at very low stress levels. (One such laboratory specimen was still deforming after 6 months at only 1.3 psi).

For clarity the creep curve is reproduced in Figure 9 to a distorted scale and the actions of the model elements associated with each part of the curve are shown below the curve. This curve really represents a family of curves with different magnitudes corresponding to different Shore hardness values and shape factors. The stress levels used are quite low (5 to 10 psi). On application of load, there is an instantaneous deformation ϵ_0 (a spring element) and then a curved section which is delayed elasticity (a Kelvin unit), a straight-line flow with time (a dashpot) up to the unload point. On removal of the load, these actions appear in reverse: an elastic snapback ($= \epsilon_0$), a delayed recovery and some permanent set.

The four-element model is the simplest model to describe the material behavior, but many authors, including Billmeyer (3), Treloar (2) and Alfrey (4), state that this is an oversimplification and should be used with caution, because it applies only to a material with a single stress relaxation time. The polymers, in general, exhibit stress relaxation but the details of the stress relaxation process depend on the multiplicity of ways in which the molecules can regain their most probable configurations. Consequently, there are so many modes of relaxation that the spectrum of relaxation times can be approximated by a distribution function. If there were but a single relaxation process, the rate of stress decay would be a simple exponential function. However, Stern and Tobolsky (5) in a specialized study of polysulfides have established that this particular polymer differs from the rest of the rubbery polymer group in that it does exhibit a single stress relaxation time. This contribution, together with the creep curve, should establish the four-element model as an adequate approximation to

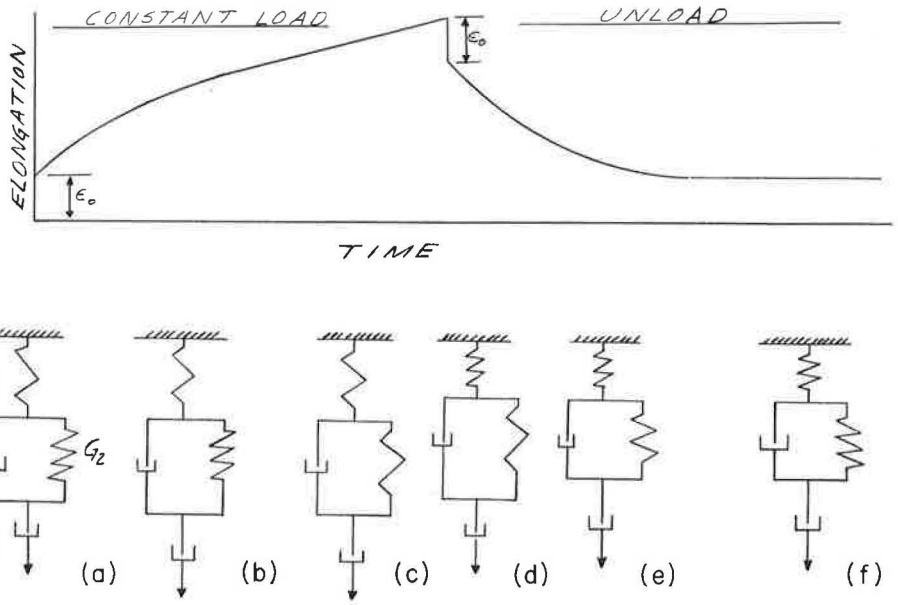

Figure 9. Model movements: (a) spring G, deformed, (b) Kelvin unit and η_3 deforming, (c) η_3 still deforming, (d) spring G, recovered, (e) Kelvin unit recovering, and (f) η_3 remains deformed.

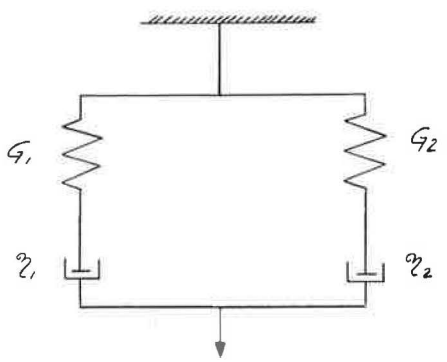

Figure 10. Equivalent model (Model B).

describe the action of the viscoelastic joint sealant under load. Strictly speaking, in a material with a true single relaxation time, no creep recovery would be expected at the termination of a stress relaxation experiment. Actually, a small amount of creep recovery was noticed but was considered not sufficient to invalidate the approximation.

The basic four-element model is excellent for demonstrating the three characteristics of polymer behavior, i.e., instantaneous elasticity, delay elasticity, and flow. This model is conveniently solved for strain when an imposed stress on the system is specified. However, for the more practical case of solving for stress under an imposed strain program, it is more convenient to substitute an equivalent model than to solve the basic model. The equivalent model shown in Figure 10 is related to the basic model through a set of equivalency equations included in Appendix B with sample problem solutions.

The basic equation for stress taken from the model is

$$\sigma = \left[\beta\eta_1 + e^{-t/\tau_1}(G_1\epsilon_o - \beta\eta_1)\right] + \left[\beta\eta_2 + e^{-t/\tau_2}(G_2\epsilon_o - \beta\eta_2)\right] \qquad (6)$$

in which

β = strain rate,

η_1, η_2 = viscous constants taken from the creep curve,

G_1, G_2 = elastic constants taken from the creep curve,

ϵ_0 = initial displacement,

τ_1, τ_2 = relaxation times (defined as the time necessary for the stress in the material to decay to 1/e times the initial stress), and

t = time.

A complete development of the stress equation has been given previously (6).

EXPERIMENTAL WORK

The materials used in this work were all two-component cold-poured polysulfide rubbers. All materials were commercial grade, in quart or gallon containers, and were donated by the manufacturers. Polysulfide joint sealants are marketed with values of Shore hardness ranging from 5 to 50. Since New York State currently specifies a Shore range from 10 to 15 for bridges and pavement joints, only those materials in and around this range were selected for test. The sealants are available in both gray and black and both types were used without distinction. The sealants were grouped into three categories by hardness: the soft range (Shore hardness 3 to 8), the medium range (8 to 16), and the hard range (16 to 22). One set of modulus tests used a material with a hardness of 30. All hardness measurements were Shore A.

In all, eight tests were conducted. Two of these were to confirm the assumptions made in Tons' paper, i.e., the constant volume assumption and the parabolic neckdown assumption. The other tests were of cycling tension and compression, creep, modulus of elasticity, stress relaxation, photoelastic correlation, and peel strength.

Flexible sealants for joints have many applications in industry which necessitate a wide range of sizes and shapes for the sealant. Since the present work was concerned with the expansion joints in bridges, only those shapes which might be applicable to this specific use were included. In all, eight sizes were included in each test, ½- and 1-in. wide specimens in joint depths of ½, 1, 1½ and 2 in. Each test was performed in each of the Shore hardness ranges and, in most cases, was repeated with materials from at least two manufacturers in each range. Thus, the creep test, for instance, would involve the testing of 16 specimens in each hardness range or 48 specimens in all.

Description of Experiments

The constant volume assumption was checked in a triaxial compression tester in the Rensselaer Soil Mechanics Laboratory. The apparatus is standard in soils work and will not be described in great detail here. It consists of a hollow plastic cylinder filled with water into which the specimen is placed. Loading is accomplished by a 1-in. diameter plunger extending through the top cover plate. A graduated tube to show differences in water level is used as a reading device.

The parabolic neckdown assumption was checked by using an Ames dial gage as a depth indicator. A sealant specimen mounted on concrete blocks was placed in the cycling machine and extended. The Ames gage was mounted in a wooden block with the plunger extending downward. The block was then placed on top of the concrete test blocks across the extended joint. The amount of neckdown of the extended sealant was read directly from the dial gage. The cycling tension and compression test was performed in a machine designed and built specially for the purpose by R. J. Schutz. Specimens for this test were prepared with concrete test blocks. Lengths of the block and, consequently, of the specimen were 3 in. and the joint depth was variable up to 2 in.

The creep test, which furnishes the constants for the stress equation, was accomplished by static loading. Specimens, 6 in. long, were formed between sections of 2

by 2-in. aluminum angles, $7\frac{1}{2}$ in. long. Creep curves, which are plots of strain vs time at constant load, were plotted for a range of shapes, loads and hardness values. The curves are included in Appendix A.

Specimens for the modulus of elasticity test were identical with the creep specimens. The test was performed in a 30,000-lb capacity pendulum-type Riehle testing machine. The modulus curves plotted by the machine in units of load vs deformation and with a change in scale only are also included in Appendix A. Strain rate for the modulus test was 0.1 in./min.

The load-deformation (or stress-strain) curves for these materials were, of course, nonlinear functions and the value of modulus used for computation was the value of stress at 100 percent strain.

The stress relaxation test yielded a plot of stress vs time at constant strain. A constant strain of 50 percent was used throughout the work. The test was performed on the same pendulum machine as the modulus test.

The photoelastic work consisted of a verification of the stress relaxation time as determined on the pendulum machine. Specimens were 1 by 1 in. in cross-section and 6 in. long. The material was a translucent polysulfide epoxy with the manufacturer's formulation adjusted to vary the Shore hardness. Creep curves were plotted and then identical specimens were tested on the pendulum machine and in the polariscope (Appendix A, Figs. 29 and 33).

The peel test used was somewhat similar to the ASTM Peel Test. The sealant was spread on 1- by 6-in. rigid substrate. A 1-in. wide strip of heavy canvas was impregnated with sealant and then placed on the substrate and rolled until the depth of sealant and canvas was $\frac{1}{16}$ in. The canvas strip was then folded back through 180° and the canvas and rigid strip were placed in opposite jaws of the pendulum machine. The rate of peel used was 3 in./min and maximum load was read directly from the machine.

DISCUSSION

The sample problems for the elastic sealant (Appendix B) illustrate that shear, when combined with extension, may be neglected for all practical purposes. However, shear in combination with compression of the sealant produces a dangerous condition. Midspan deflection of a bridge structure is shown to produce practically no shear but does increase the tensile strains in the sealant by as much as 25 percent.

Leadermann (7) describes time as the main character in his work on creep of polymers. This same description might be paraphrased by stating that in dealing with joint sealants, time has been the forgotten parameter. The sample problems shown in Appendix B indicate that when time, or better stated, when stress relaxation enters the picture, stresses in the sealant drop to almost negligible values. The problem then becomes one of shape and recovery rather than stress.

In addition to the tests mentioned previously, curves included in Appendix A show the variation of hardness with temperature and the variation of modulus of elasticity with hardness. All experimental work in the present investigation was done at room temperature and these curves mentioned are an attempt to extrapolate these results to other temperature values. For example, if it is desired to use a sealant which has a hardness of 5 at room temperature for some application at -30 degrees its behavior can be predicted. At this temperature, the A-5 material has a hardness of 20. The creep, modulus of elasticity and stress relaxation values can be found from the respective curves for the A-20 material. This extrapolation method is admittedly a limitation on the present study but it represents at least a starting point for predictability.

The creep curves included afford a measure of creep predictability. The higher modulus materials show a much better compliance with the creep curve shape than the softer materials. All curves are shown as smooth curves, but the softer materials are quite erratic in behavior, and the curves represent the average of many retests and the elimination of some obviously faulty values.

It must be remembered that when a structure moves, the forces exerted on the sealant are quite high and the sealant must comply with the imposed strain program.

It may seem ridiculous to state that the sealant never moves the structure, but at this time many spalling failures are blamed on the sealant because it pulled the concrete apart. The values of creep, modulus and stress relaxation included here should help to dispel this notion. A spalling failure is simply due to poor concrete, not a strong sealant.

The creep behavior does vary with shape. Under equal stresses, a shallow seal will creep more than a deep one. This result is not surprising when compared to the parabolic length of the sealant. It is also important that within the 200 percent strain limitation the creep curve will superimpose when subjected to a variation in stress. More research is needed to determine whether the new polysulfide formulations show any tendency towards work hardening under repeating cycling.

The modulus curves are purposely left in terms of load vs elongation to make them easily readable. When plotted as nominal stress-strain curves (stress based on original cross-sectional dimensions), they are virtually coincident which shows that modulus values are practically independent of shape. The modulus value by definition is stress at 100 percent strain. The modulus values are plotted for a strain rate of 0.1 in./min. They will vary with strain rate because the steep gradient of the modulus curve at the beginning of the test corresponds to the steep downward gradient of the stress relaxation curve for very short times.

No values of ultimate cohesive strength are reported because of the fear of erroneous interpretation. Every sealant tested was extended well beyond 200 percent strain, and some as far as 1,000 percent, before failure. Above 200 percent strain neckdown is no longer parabolic and cross-sectional area reduces to almost zero. Consequently, any stress (which is load divided by area) would show values so high that they appear ridiculous.

The stress relaxation curves are perhaps the main contribution that this paper has to offer. The curves follow a generally exponential shape. Tobolsky (5) has shown that the polysulfides in general follow the relation:

$$f = f_0 \exp -k't \tag{7}$$

He states that the curve is, in general, steeper than exponential and relates k' to the rate of bond rupture. His method for finding k' is a curve-fitting technique. The experimental curves offered here are also steeper than exponential and a curve-fitting scheme is also used. The equation which fits the curve is really a family of equations of the form:

$$f = f_0 \exp (t/\tau)^n \tag{8}$$

in which n varies with τ. For low values of τ (about 1 hr), n approaches unity. For higher values of τ, n varies between 0.5 and 1.0. The highest value of τ obtained in this work was 6 hr. This was for a high modulus sealant. The middle range (A-12) sealants showed a relaxation time of 3 hr. The erratic soft-range materials showed great variation in values and also wide variation for single points on each curve. Further study of stress relaxation should lead to a definitive relationship by which τ and n could be predicted for different sealants.

The important fact to be recognized with polysulfide sealants is the order of magnitude of the stress relaxation time. In just a few hours after an imposed strain, the stress has relaxed to less than half of its initial value. The fact that the relaxation is steeper than exponential is also noteworthy. In the event of an imposed strain (ϵ_0) of large value, the sealant can actually relieve the stress by as much as one-third within the first 20 min.

The peel test used was, to some extent, new and needs refinement. The test specimens, 1 in. wide by 6 in. in gage length, were $\frac{1}{16}$ in. thick. Eleven of the twelve specimens tested did not actually fail by peeling away clean from the substrate but by

tearing of the sealant. The average value of tearing strength was 42.5 lb for the 1-in. wide strip at a testing machine rate of 3 in./min. This value is very close to the values of peel strength and tear resistance which are available from the various manufacturers. Further work on the peel test should include an investigation of the effect of specimen thickness and also a long-time test at low loads, somewhat after the fashion of the Bikerman (8) test.

The results of the photoelastic work have to be classed as both good and poor. The original intention was to find a birefringent material with the same properties as the actual sealant to make a comparative study. Finally, several formulations of epoxy-polysulfide combinations were developed in the desired hardness ranges, but these showed a shorter relaxation time, a faster creep rate and more permanent set than the actual sealants. Differences were expected, of course, but it was hoped that a proportionality constant could be derived such that actual stresses in a sealant could be checked by photoelasticity. However, the characteristics of the photoelastic material are somewhat contradictory when compared to sealant behavior. More research is needed to determine the factor which can be applied to the two materials so that a quantitative prediction can be made.

The success achieved with the photoelastic method was the development of several materials which exhibit stress relaxation according to an exponential law. Identical specimens of material were tested in the Riehle machine and the polariscope; both of these tests show very good agreement with the theoretical curve. Quantitative values for the photoelastic curve were obtained by counting the total number of stress fringes which passed a given point during the rapid loading process and equating this fringe order to the maximum load value shown by the testing machine. One end of the specimen was blocked at a constant 1 in. width and the other end of the specimen was strained to 25 percent. This method of obtaining clear fringes assumes a linearity of stress in the specimen. This linearity should be checked by strain gaging if the method is to be used further.

Since so much emphasis has been placed on shape, some new shapes were tested to find one which would not extrude above the roadway surface. Two such shapes are shown in Figure 11. The trapezoidal joint would help to eliminate spalling failures, but it also makes a wider joint and, consequently, would cause a car to make an objectionable thump when riding over the joint. When formed with a flush top, this joint extrudes above the roadway surface, but not in a parabolic shape, under compression loading. When formed with a slight depression in the surface, the sealant no longer extrudes under compression, but the poor riding quality is still objectionable.

The hollow shape shown in Figure 11 is actually formed by filling the joint to half depth, inserting a dumbbell-shaped strip of soft urethane foam, and then filling the joint. For wide joints (1 in. and wider) such as might be encountered in bridge work, this shape has possibilities. However, because it is difficult to form and the foam has a tendency to float, the few specimens tested showed rather erratic behavior. These problems might be solved by experiment and experience.

The ordinary rectangular shape formed with a depression in the top also offers possibilities. This shape does not extrude above the roadway for shallow joints. Deeper joints do tend to bulge upward under compressive loads.

RECOMMENDATIONS

Although the polysulfide sealants have many properties which make them desirable as sealants, such as high bond strength, extensibility, and excellent short-term mem-

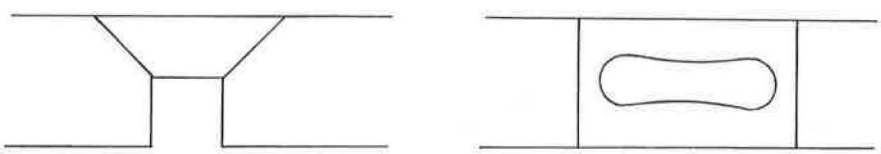

Figure 11. Experimental joint shapes.

ory, the sealant problem is not yet solved. There are many aspects of sealant behavior that have not yet been investigated. Among the many questions still to be answered are the following:

1. What effect does work hardening have on the physical properties of a sealant?
2. Does the aging and weathering of a sealant affect its mechanical behavior?
3. What is the response of a sealant in a skewed expansion joint?

A great deal of additional research is necessary so that these and other vital questions may be answered, not only in terms of the polysulfides, but also with the other available sealant materials.

ACKNOWLEDGMENTS

The complete study from which this paper was taken was presented as a Doctoral Dissertation at Rensselaer Polytechnic Institute. The author wishes to extend his thanks to Professors Egons Tons, J. F. Throop, J. T. Watkins, J. Hollingsworth, R. H. Trathen and R. M. Lewis for their encouragement and direction.

The joint sealant industry on the whole has been very helpful. Particular thanks are extended to Raymond Schutz, Sika Chemical Corp.; C. A. Peters, Allied Materials Corp.; Norbert Hochreiter, H. B. Fuller Co.; Joseph Amstock, Products Research Corp.; Aaron Kaplan, Lewis Asphalt Engineering Co.; H. V. Wittenwyler, Shell Chemical Co.; and A. Shuman, Polarizing Instrument Co.

The author's deepest debt is to Harold B. Britton of the New York State Department of Public Works, without whose constant faith, encouragement and material assistance the project never could have been undertaken.

REFERENCES

1. Tons, E. A Theoretical Approach to Design of a Road Joint Seal. Highway Research Board Bull. 229, pp. 20-53, 1959.
2. Treloar, L. R. G. The Physics of Rubber Elasticity. Oxford Univ. Press, 1958.
3. Billmeyer, F. W. Textbook of Polymer Chemistry. New York, Interscience Publishers, 1957.
4. Alfrey, T. Mechanical Behavior of High Polymers. New York, Interscience Publishers, 1948.
5. Stern, M. D., and Tobolsky, A. V. Stress Relaxation in Polysulfide Rubbers. J. Chem. Phys., Vol. 14, No. 93, 1946.
6. Cook, John P. A Study of the Action of Elastic Joint Seal Materials in the Expansion Joints of Bridge Decks. Doctoral Diss. Rensselaer Polytechnic Inst., Dept. of Civil Eng., 1963.
7. Leadermann, H. Elastic and Creep Properties of Filamentous Materials and Other High Polymers. Washington, D. C., Textile Foundation, 1943.
8. Bikerman, J. J., and Yap, W. Rheology of Peeling in a Newtonian Liquid. Trans. Soc. of Rheology, Vol. 2, pp. 9-21, 1958.

Appendix A

GRAPHICAL RESULTS

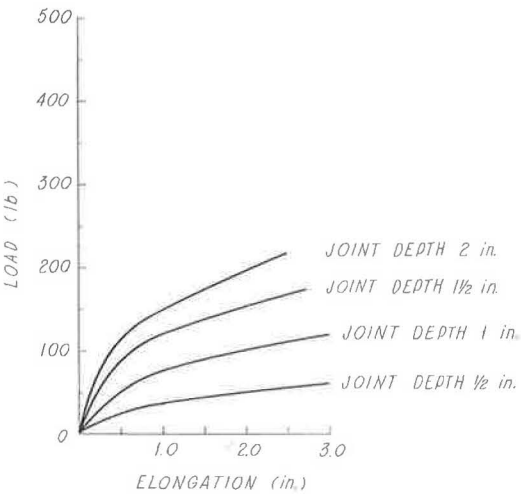

Figure 12. Load elongation curves; Shore A-5, $\frac{1}{2}$-in. wide joint.

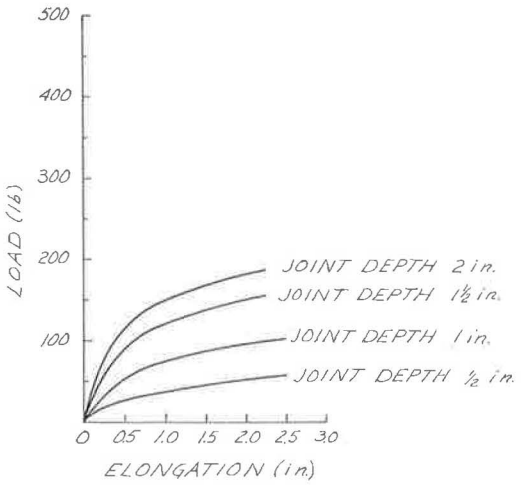

Figure 13. Load elongation curves; Shore A-5, 1-in. wide joint.

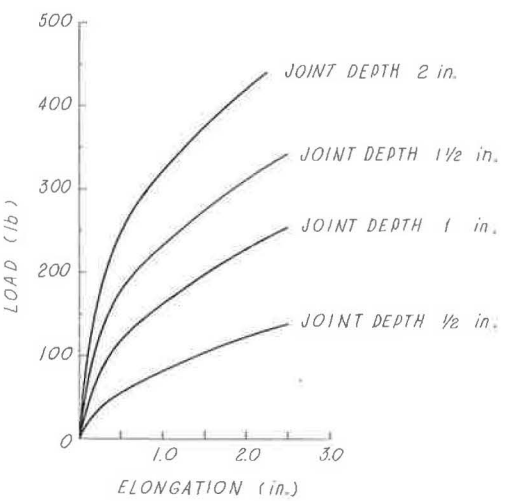

Figure 14. Load elongation curves; Shore A-12, $\frac{1}{2}$-in. wide joint.

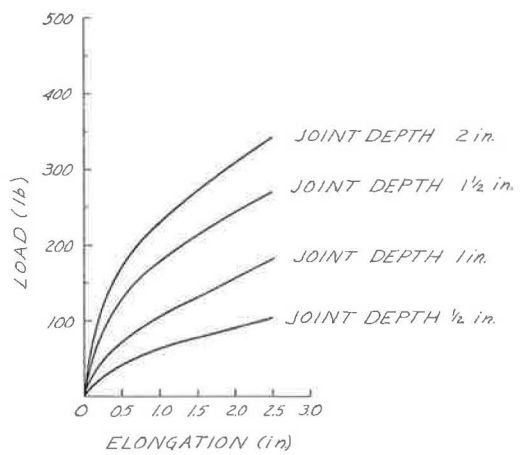

Figure 15. Load elongation curves; Shore A-12, 1-in. wide joint.

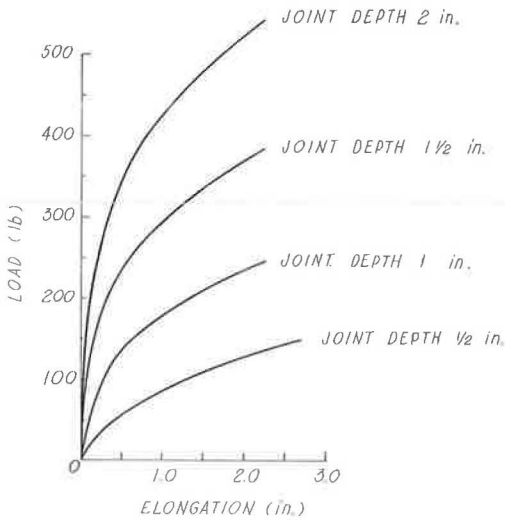

Figure 16. Load elongation curves; Shore A-20, $\frac{1}{2}$-in. wide joint.

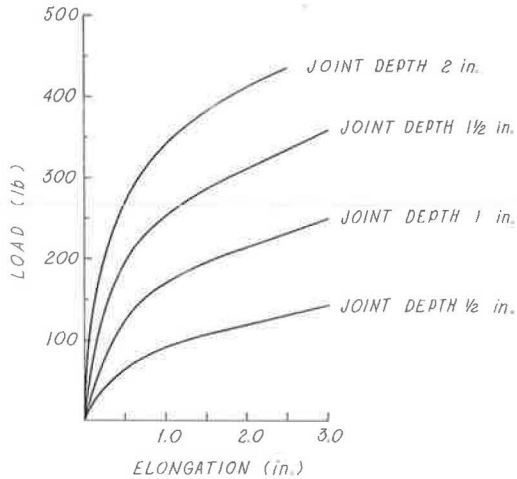

Figure 17. Load elongation curves; Shore A-20, 1-in. wide joint.

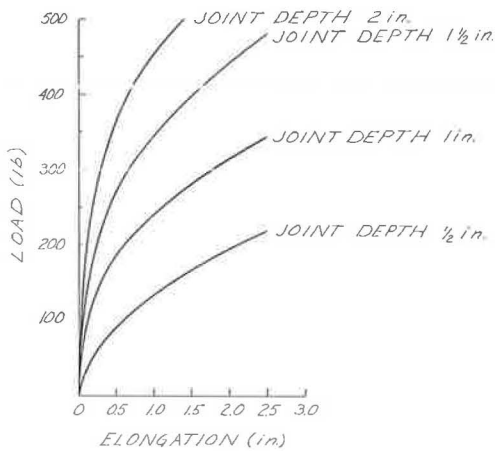

Figure 18. Load elongation curves; Shore A-30, $\frac{1}{2}$-in. wide joint.

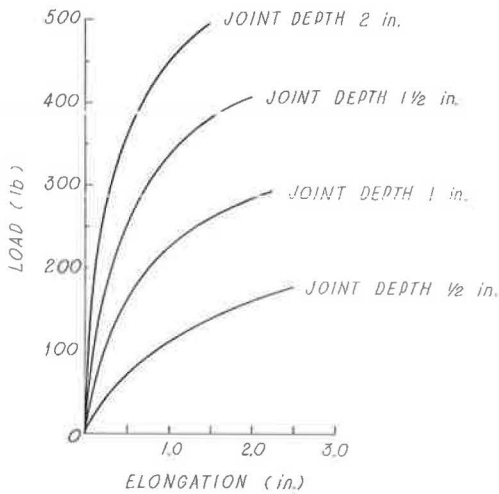

Figure 19. Load elongation curves; Shore A-30, 1-in. wide joint.

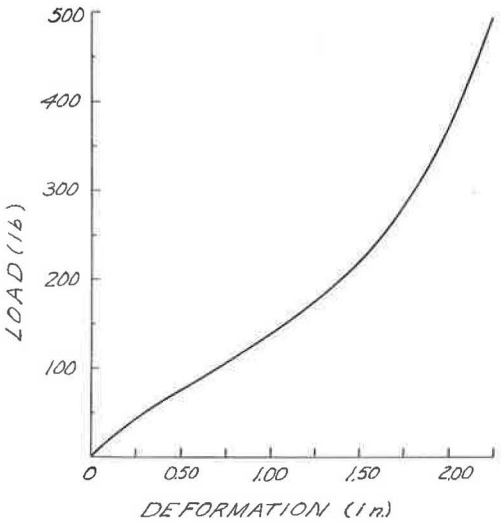

Figure 20. Load-deformation curve—compression; Shore A-12, $3\frac{1}{2}$-in. diameter, 4-in. high specimen.

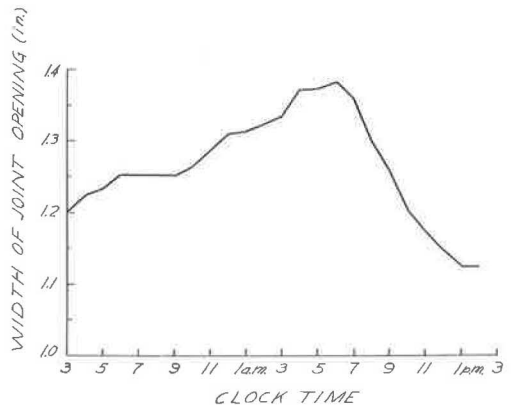

Figure 21. Rate of bridge movement; normal joint width 1in. at 76 F, 100-ft bridge span, 22 to 66 F temperature variation.

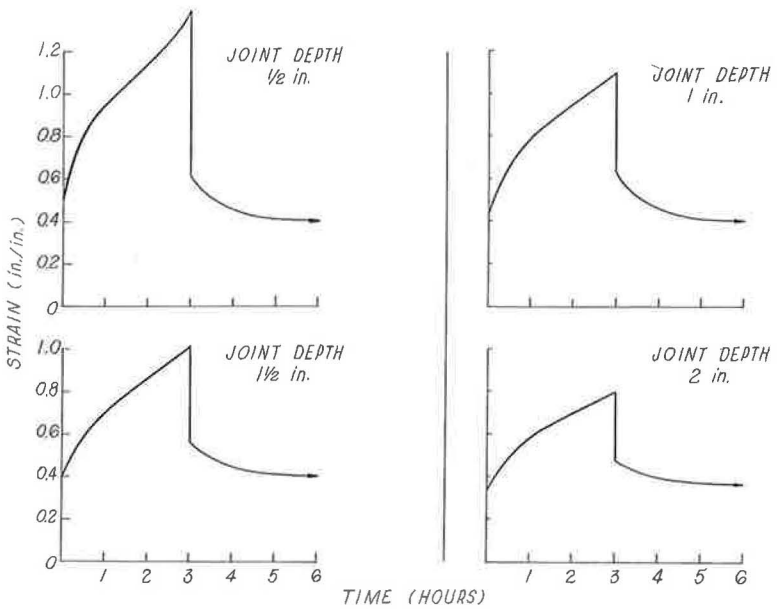

Figure 22. Creep curves; Shore A-5, $\frac{1}{2}$-in. wide joint, 8-psi constant load.

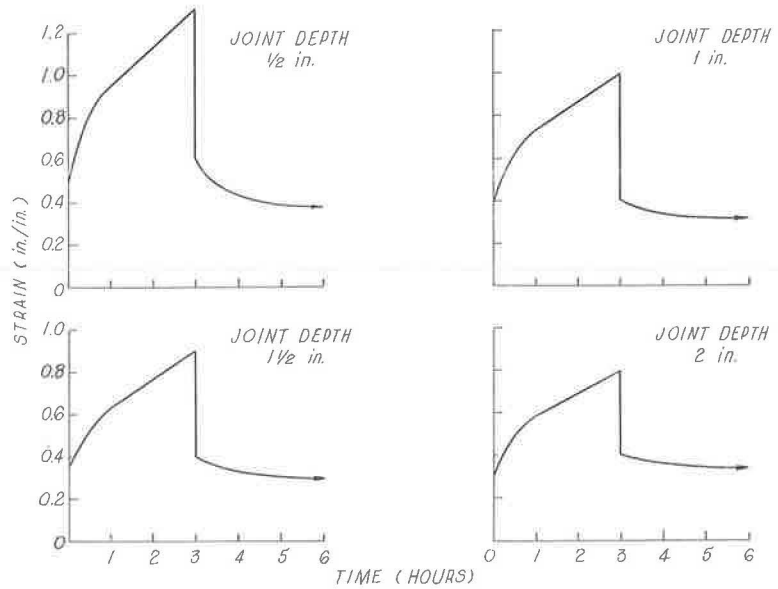

Figure 23. Creep curves; Shore A-5, 1-in. wide joint, 4-psi constant load.

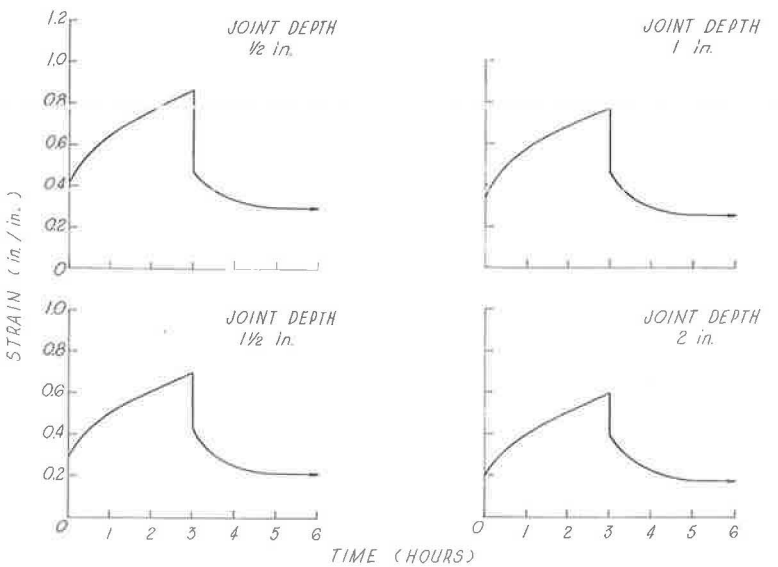

Figure 24. Creep curves; Shore A-12, $\frac{1}{2}$-in. wide joint, 12-psi constant load.

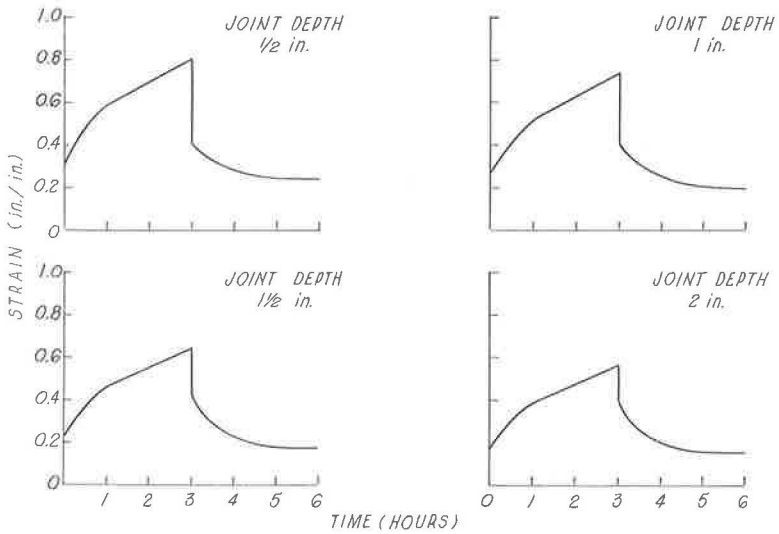

Figure 25. Creep curves; Shore A-12, 1-in. wide joint, 6-psi constant load.

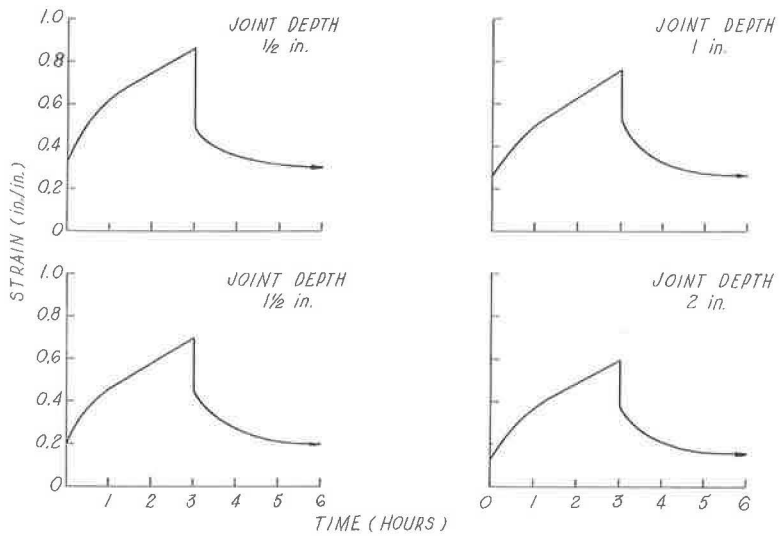

Figure 26. Creep curves; Shore A-20, $\frac{1}{2}$-in. wide joint, 16-psi constant load.

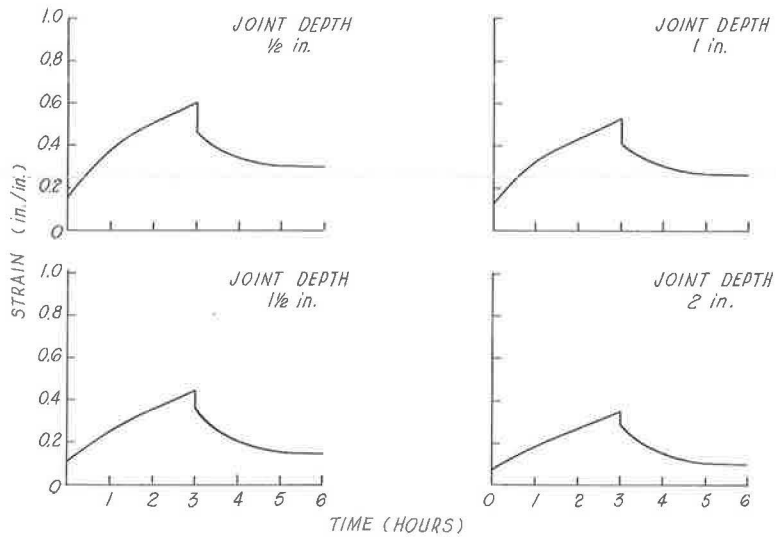

Figure 27. Creep curves; Shore A-20, 1-in. wide joint, 8-psi constant load.

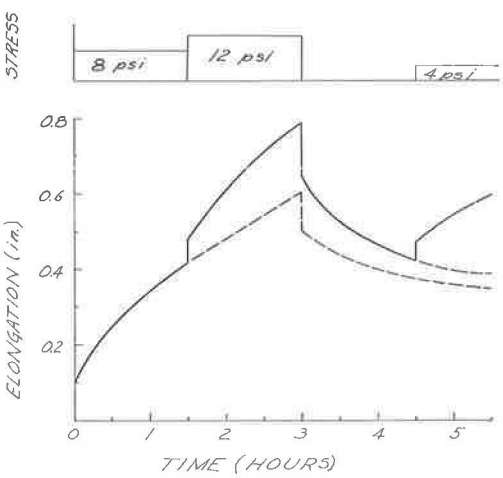

Figure 28. Boltzmann superposition curve; Shore A-12, 1-in. wide joint.

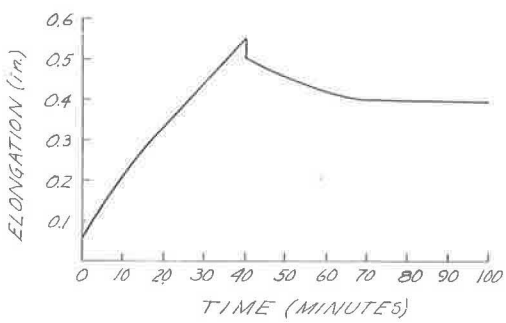

Figure 29. Creep curve—photoelastic specimen of clear polysulfide epoxy; Shore A-20, 1- by 1- by 6-in. specimen.

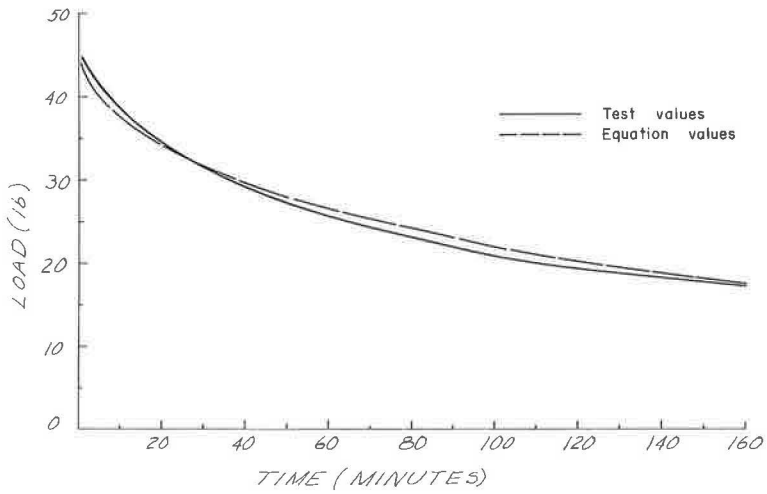

Figure 30. Stress relaxation curves; Shore A-5, $f = f_o \exp (t/\tau)^{0.6}$ where $\tau = 180$ min.

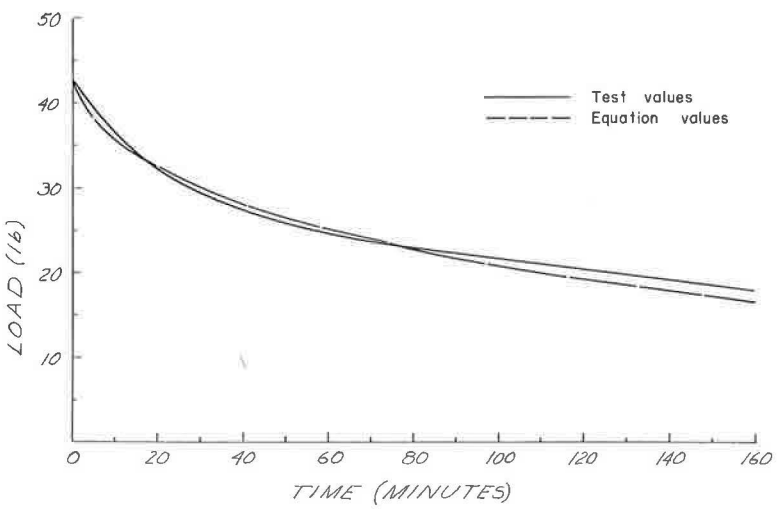

Figure 31. Stress relaxation curves; Shore A-12, $f = f_o \exp (t/\tau)^{0.6}$ where $\tau = 180$ min.

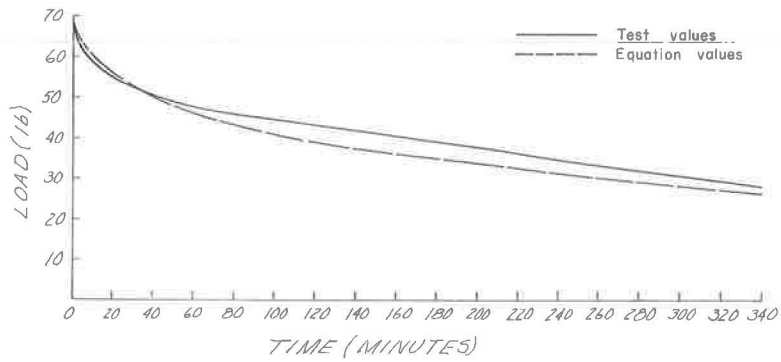

Figure 32. Stress relaxation curves; Shore A-20, $f = f_o \exp -t/\tau)^{0.5}$ where $\tau = 360$ min.

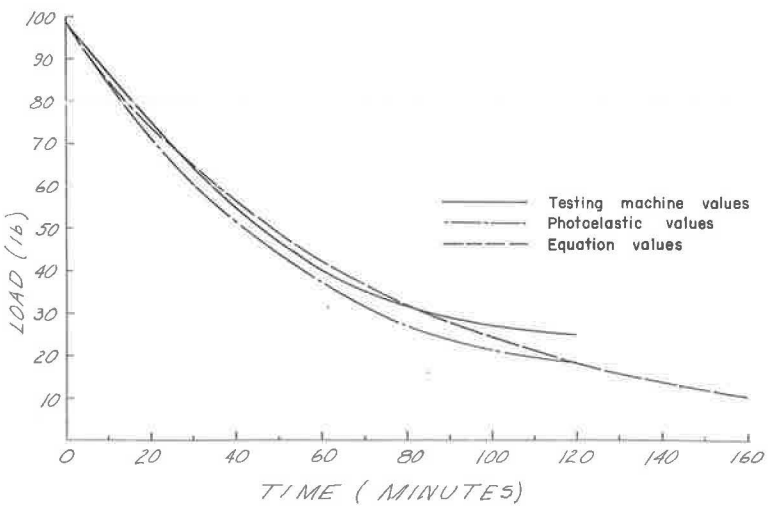

Figure 33. Stress relaxation curves--photoelastic specimen of clear polysulfide epoxy; Shore A-20, 1- by 1- by 6-in. specimen, 25 percent constant strain.

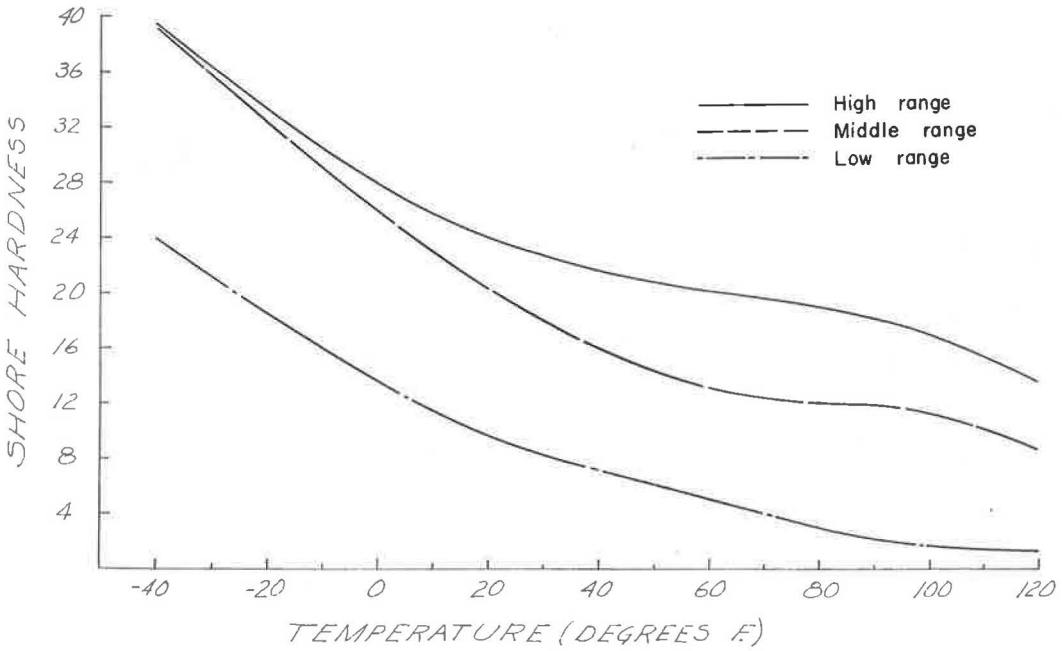

Figure 34. Shore hardness vs temperature.

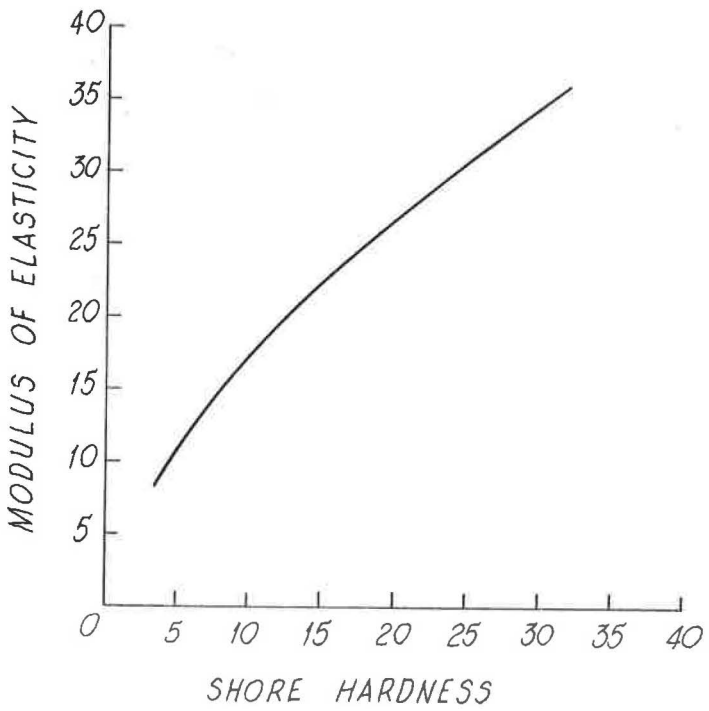

Figure 35. Tensile modulus vs Shore hardness.

Appendix B

SOLUTION OF SAMPLE PROBLEMS

Sealant as an Elastic Material

To cover the range of field conditions, three cases of stress should be considered: (a) tension (or compression) alone, (b) tension plus shear, and (c) compression plus shear. For purposes of illustration, dimensions of a typical highway bridge are used. The structure is a 60-ft span rolled-beam bridge with a concrete deck. The beams are 33WF130 spaced at 6 ft cc. The joint sealant is a square cross-section, 1 in. wide by 1 in. deep.

Tension Alone.—Assume the sealant material is placed at 75 F. Temperature range is -40 to +120 F, maximum differential is 75 - (-40) = 115, and coefficient of expansion of bridge is 0.0000065 (steel). Anticipated movement = 0.0000065 × 60 × 115 × 12 = 0.54 in. due to temperature.

Tension Plus Shear.—The case of tension plus shear could be caused in two ways, first by the impact of a truck wheel bearing on the extreme end of the bridge, or rotation at the support as caused by midspan deflection. A truck wheel bearing on the extreme end of the bridge tends to deflect the short cantilevered portion of the bridge which extends beyond the centerline of bearing (assumed to be 1 ft). For a 20-ton truck, one rear wheel = W(0.4) = 0.4 × 20 × 2 = 16 kips, distribution factor (AASHO) = S/5.5 = 6.0/5.5 = 1.09. Impact at 30 percent is given by P = 16 × 1.09 × 1.3 = 22.7 kips. Assume this load is concentrated at the end of the short cantilever; therefore,

$$\text{Deflection} = \frac{PL^3}{3EI} = \frac{22.7 \times (1)^3 \times 1728}{3 \times 29 \times 10^3 \times 6700} = 0.000067 \text{ in.}$$

This deflection represents a shear-type movement in the sealant but its magnitude is only one-ten thousandth of the movement in the tensile direction; therefore, shear can be neglected. To consider the end rotation of the structure, consider the 20-ton truck at midspan, using the same distribution factor and impact. Therefore, P = 20 × 1.09 × 1.3 = 28.4 kips, and end rotation θ is given by:

$$\theta = \frac{PL^2}{16EI} = \frac{28.4 \times 60^2 \times 144}{16 \times 29 \times 10^3 \times 6700} = 0.0047 \text{ rad}$$

Movement at top of slab = 45 × 0.0047 = 0.213 in.; top Wx = length at top of extended sealant = 1.54 + 0.213 = 1.753 in. For the amount of rotation shown (0.0047 rad), the upward movement at the end of the slab will be 0.060 in. This is a shear-type movement but it is only $^{8}/_{100}$ of the movement in the tensile direction and makes virtually no change in the stress magnitude.

The implication of these computations is that shear may, in general, be neglected in combination with tension, but that the case of end rotation is important. However, this importance comes, not from shear, but from the fact that it causes a further extension of the sealer in the tensile direction, which in this case is almost one-half as much (0.213 vs 0.54) as the extension caused by temperature change. This fact should be given careful consideration in the future design of the service life of any joint sealer.

Using the statistical approach, the stresses in the sealant are determined as follows:

Total extension = 0.54 + 0.213 = 0.753 in.
Joint width = 1.0 + 0.753 = 1.753
$\lambda_1 = \lambda = 1.753/1.0 = 1.753$
$\lambda_2 = 1/\lambda = 1/1.753 = 0.570$
$\lambda_3 = 1$
$W = {}^{1}/_{2}\, G\left[\lambda^2 = 1/\lambda^2 + 1 - 3\right]$

The only force acting is in the tensile direction; therefore,

$$f = \frac{dw}{d\lambda} = G\left[\lambda - \frac{1}{\lambda^3}\right]$$

The value of G (34 psi) is in the value for a high modulus tread stock rubber which is as hard a material as could be practicably used as a sealant:

$$f = 34\left[1.753 - \frac{1}{(1.753)^3}\right] = \left[1.753 - 0.185\right] 34 = 53.3 \text{ psi}$$

This force f is the magnitude of the force acting on a unit cross-sectional area in the unstrained state. For this specific problem it is acting adjacent to the bonding surface where no neckdown has taken place. This value at the interface must be related to the peel strength of the material in question. The polysulfides show a peel strength which averages only 42 psi by test, so that a peel failure seems imminent. The stress "t" on the necked-down cross-section of the sealant is given by:

$$t_1 = \lambda_1 f_1 = 1.753 f_1 = 93.5 \text{ psi}$$

Comparison of this value with the true stress-true strain curve indicates that a polysulfide will stand stresses of three times this magnitude at this strain before failure. In brief, cohesion looks safe but a peel failure seems imminent.

Compression Plus Shear.—Separate from, but related to, these examples is the case at the other end of the temperature scale. When the bridge is fully expanded and the sealer is compressed, the latter extrudes above the roadway surface. At this time, temperature is high and the sealant has softened somewhat. Experience shows that these conditions normally result in failure by folding and flattening of the sealant under the action of traffic. However, since we are working under the assumption that the sealant is fully elastic, the net effect of traffic will be the depression of the sealant back into the joint. The stress in the sealant at this time will be the resultant of a compressive stress caused by temperature and a punching type of shear as caused by the wheel load. Movement due to compression = $(1.20 - 75) \times 0.0000065 \times 60 \times 1.2 = 0.21$ in. due to temperature;

$$\lambda_1 = \frac{1 - 0.21}{1.0} = 0.79$$

$$f = \frac{dw}{d\lambda} = G\left[\lambda - \frac{1}{\lambda^3}\right] = 34\left[0.79 - \frac{1}{(0.79)^3}\right] = 42.5 \text{ psi}$$

The amount of shear is determined by writing and differentiating the parabolic equation of the extruded sealant. For this case shear is the downward movement back into the joint of a differential element of sealant adjacent to the interface. It is expressed as the tangent of the angle ϕ which the sealant makes with the pavement: $\alpha = \tan \phi = 0.47$ and shearing stress $\gamma = G\alpha = 34\,(0.47) = 15.9$ psi. Combining the direct compression stress with the shearing stress gives a principal stress, S max = 47.7 psi. This stress, which because of the nature of the loading is related to peel strength, also exceeds the peel strength of the polysulfides.

Sealant as a Flowing Solid

The illustrative problems use the following equivalent model equations (model shown in Fig. 10):

$$G_1^A = G_1^B + G_2^B \tag{9}$$

$$G_2^A = \frac{G_1^B G_2^B \left(\eta_1^B + \eta_2^B\right)^2 \left(G_1^B + G_2^B\right)}{\left(\eta_1^B G_2^B - \eta_2^B G_1^B\right)^2} \tag{10}$$

$$\eta_2^A = \eta_1^B \eta_2^B \frac{\left(G_1^B = G_2^B\right)\left(\eta_1^B + \eta_2^B\right)}{\left(\eta_1^B G_2^B - \eta_2^B G_1^B\right)^2} \tag{11}$$

$$\eta_3^A = \eta_1^B + \eta_2^B \tag{12}$$

The data for these problems were taken from the creep and stress relaxation curves included here for the medium range material (Shore A = 12). The strain rate is taken from a curve of joint movement with temperature change. Hourly fluctuations of temperature were obtained from the U. S. Weather Bureau. The temperature curves are plotted for the one day in March which showed the greatest temperature variation. According to this curve, the rate of temperature change and, consequently, the strain rate remain relatively constant for a period at 0.0014 in./in./min.

The following data were taken from the creep curve for Model A:

$$G_1^A + \frac{1}{3} E_1^A = 10 \text{ psi}$$

$$G_2^A = \frac{1}{3} E_2^A = 7 \text{ psi}$$

$$\eta_2^A = 960 \text{ lb-min/sq in.}$$

$$\eta_3^A = 9,600 \text{ lb-min/sq in.}$$

From the equivalency relations, the constants for Model B are

$$G_1^B = 7.0 \text{ psi}$$

$$G_2^B = 3.0 \text{ psi}$$

$$\eta_1^B = 9,300 \text{ lb-min/sq in.}$$

$$\eta_2^B = 300 \text{ lb-min/sq in.}$$

$$\tau_1 = \frac{\eta_1}{G_1} = 1,330 \text{ min}$$

$$\tau_2 = \frac{\eta_2}{G_2} = 100 \text{ min}$$

Since a bridge will normally build up stress until it lurches in a sudden movement, this amount of movement will have to be assumed. This amount of lurch (ϵ_o) assumed is 0.25 in., slightly more than half the anticipated movement in a day's time.

Case I.—Where $\epsilon = \epsilon_o + \beta t$, determine the stress at t = 60 min after an initial lurch of 0.25 in.

$$\sigma = \left[\beta\eta_1 + \exp - t/\tau_1 (G_1 \epsilon_o - \beta\eta_1)\right] + \left[\beta\eta_2 + \exp - t/\tau_2 (G_2 \epsilon_o - \beta\eta_2)\right]$$

$$= \left[0.0014\,(9300) + e^{-0.066}\,(7.0 \times 0.25 - 0.0014 \times 9300)\right] + \left[0.0014\,(300) + e^{-0.60}\,(3.0 \times 0.25 - 0.0014 \times 300)\right]$$

$$= 13.02 + -11.6 + 0.42 + 0.18 = 1.92 \text{ psi}$$

Case II.—In the event that the bridge does move ideally, $\epsilon_o = 0$. The stress at t = 60 min reduces to

$$\sigma = \left[\beta\eta_1 (1 - e^{-t/\tau_1})\right] + \left[\beta\eta_2 (1 - e^{-t/\tau_2})\right]$$

$$= 13.02\ (1 - e^{-0.066}) + 0.42\,(1 - e^{-0.60}) \cong 0$$

Case III.--In the event that the bridge moves through an initial lurch and then remains at a constant elongation, $\beta = 0$ $\epsilon_o = 0.25$ and t = 60 min:

$$\sigma = \left[G_1 \epsilon_o e^{-t/\tau_1}\right] + \left[G_2 \epsilon_o e^{-t/\tau_2}\right]$$

$$= \left[7.0 \times 0.25 \times e^{-0.066}\right] + \left[3.0 \times 0.25 \times e^{-0.60}\right]$$

$$= 1.80 + 0.41 = 2.21 \text{ psi.}$$

It becomes immediately apparent that when stress relaxation enters the picture, the entire outlook changes. The stresses shown here are well below the demonstrated peel strength of the polysulfides; therefore, under normal conditions, the sealant should not fail.